Title
Nd:YAG laser irradiation in conjunction with cryogen spray cooling induces deep and spatially selective photocoagulation in animal models

Journal
Physics in Medicine and Biology, 42(2)

ISSN
0031-9155

Authors
Anvari, Bahman
Tanenbaum, B Samuel
Hoffman, Wendy
et al.

Publication Date
1997-02-01

DOI
10.1088/0031-9155/42/2/001

Phys. Med. Biol. **42** (1997) 265–282. Printed in the UK PII: S0031-9155(97)76776-9

Nd:YAG laser irradiation in conjunction with cryogen spray cooling induces deep and spatially selective photocoagulation in animal models

Bahman Anvari†‡¶, B Samuel Tanenbaum‡, Wendy Hoffman§, Samireh Said§, Thomas E Milner†‖, Lih-Huei L Liaw† and J Stuart Nelson†§

† Beckman Laser Institute and Medical Clinic, University of California, Irvine, CA, USA
‡ Department of Engineering, Harvey Mudd College, Claremont, CA, USA
§ Department of Dermatology, School of Medicine, University of California, Irvine, CA, USA
‖ Department of Physics, Harvey Mudd College, Claremont, CA, USA

Received 30 July 1996, in final form 24 October 1996

Abstract. Successful laser treatment of haemangiomas requires selective photocoagulation of subsurface targeted blood vessels without thermal damage to the overlying epidermis. We present an *in vivo* experimental procedure, using a chicken comb animal model, and an infrared feedback system to deliver repetitive cryogen spurts (of the order of milliseconds) during continuous Nd:YAG laser irradiation. Gross and histologic observations show deep-tissue photocoagulation is achieved, while superficial structures are protected from thermal injury due to cryogen spray cooling. Experimental observation of epidermis protection in chicken comb animal models suggests selective photocoagulation of subsurface targeted blood vessels for successful treatment of haemangiomas can be achieved by repetitive applications of a cryogen spurt during continuous Nd:YAG laser irradiation.

1. Introduction

Successful application of certain thermally mediated therapeutic procedures in multi-layered composite tissue is based on selective destruction of specific subsurface targets without damaging the overlying structures. For example, laser treatment of vascular lesions such as port wine stains (PWSs) and haemangiomas requires selective photothermal destruction of dilated cutaneous blood vessels while preserving the overlying epidermis.

Surface cooling with ice or water has been used as a method to prevent laser induced thermal injury to the epidermis (Gilchrest *et al* 1982, Berlien *et al* 1987, Dreno *et al* 1985, Chess and Chess 1993, Werner *et al* 1995). Although this method has been shown to be effective, cooling exposures on the order of several seconds or minutes reduce the temperature of the underlying targeted blood vessels (Anvari *et al* 1995a, Nelson *et al* 1995). Consequently, incident laser energy is utilized ineffectively by first rewarming the blood vessels to their initial temperature before sufficient heat is generated to induce photocoagulation.

Some investigators have studied the effectiveness of delivering a short spurt (of the order of milliseconds) of a cryogen to cool selectively the epidermis without reducing temperature

¶ Corresponding author: Bahman Anvari, PhD, Beckman Laser Institute and Medical Clinic, 1002 Health Sciences Road East, University of California, Irvine, CA 92715, USA. E-mail address: banvari@bli.uci.edu

0031-9155/97/020265+18$19.50

of the underlying targeted blood vessels (Anvari *et al* 1995b, c, Sturesson and Andersson-Engels 1996). When used in conjunction with flashlamp pumped pulsed dye laser irradiation for treatment of vascular lesions, use of cryogen spray cooling (CSC) has been demonstrated to prevent skin textural changes that result from thermally induced epidermal injury while allowing blanching of PWSs (Nelson *et al* 1995, 1996). In the absence of CSC, epidermal necrosis and subsequent skin textural changes have been observed when treatments are administered with equivalent laser irradiation parameters.

Haemangiomas are vascular tumours, characterized by rapid cellular proliferation, which may infiltrate the entire dermis and extend several millimetres in depth (Mulliken and Young 1988). Although laser irradiation has been used to induce photothermal destruction of haemangiomas, thermal damage to the epidermis and papillary dermis remains a concern. CSC in conjunction with laser irradiation may offer a means to protect superficial tissue structures while achieving deep photocoagulation of thick haemangiomas.

In a previous study, utilizing *ex vivo* rabbit liver tissue, we demonstrated deep-tissue photocoagulation can be induced by continuous Nd:YAG laser irradiation while protecting the superficial tissue by CSC (Anvari *et al* 1996). Approximately 5 mm of tissue was photocoagulated, while protecting 400 μm of superficial structures from thermal injury when using specified laser irradiation and CSC parameters.

To further investigate the effectiveness of CSC in protecting superficial tissue structures while achieving deep-tissue photocoagulation with the Nd:YAG laser, we report results of an *in vivo* experiment utilizing the chicken comb animal model. An analysis of the frequency of CSC during and after laser irradiation, and clinical implications for treatment of haemangiomas, are discussed.

2. Materials and methods

The highly vascular chicken comb was used as a model for haemangiomas since its histoanatomy is analogous to that found in selected vascular birthmarks, and has been extensively studied (Orenstein *et al* 1990). Seven adult female leghorn chickens were anaesthetized by intramuscular injection of 0.3 ml ketamine and xylazine in a 9:1 volumetric ratio 10–15 min prior to the beginning of each experiment. Experimental protocol and handling of the animals were approved by the Animal Research Committee at the University of California, Irvine.

The experimental set-up for laser irradiation and CSC is shown in figure 1. Laser light was delivered through a 600 μm core diameter silica multimode optical fibre, and directly incident onto the comb. Three ranges of power levels (low, intermediate, and high) were selected (table 1). Irradiation times of the order of tens of seconds were used to achieve a large volume of photocoagulated tissue. The diameter of the laser irradiated site, d, was maintained at 7 mm in all experiments. Depending on the size of the comb, three to 11 sites were irradiated; combs with smaller areas allowed fewer irradiation sites.

Laser irradiation and CSC parameters utilized on each comb are summarized in table 2. Chlorodifluoromethane (Aldrich Chemical Company, Milwaukee, WI; boiling point (BP) $\approx -40\,^{\circ}$C), a hydrochlorofluorocarbon (HCFC-22), and tetrafluoroethane (ICE KLEA, Wilmington, DE; BP $\approx -26\,^{\circ}$C), a hydrofluorocarbon (HFC-134a) were used as cryogens on five and two chicken combs, respectively, to examine the influence of BP in protecting tissue superficial structures during laser irradiation. HFCs do not contain chlorine, and therefore, have no ozone depleting potentials (Manzer 1990). HCFCs have relatively minimal ozone depleting potentials as compared to chlorofluorocarbons (Manzer 1990, Kanakidou *et al* 1995).

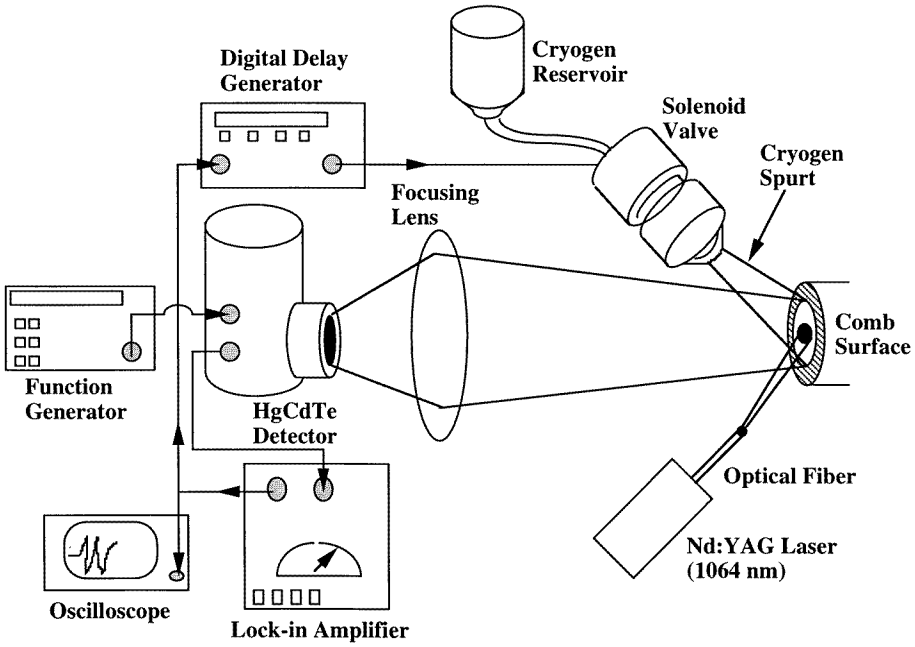

Figure 1. A schematic diagram of the experimental apparatus for CSC and Nd:YAG laser irradiation. Measurement of surface temperature is made by infrared radiometry.

Table 1. Laser irradiation parameters used in the experiments. The diameter of the laser irradiated spot was 7 mm in all experiments.

Power level	Delivered laser power, P (W)	Irradiation time, t_{irrad} (s)	Radiant exposure, E (J mm^{-2})
Low	5	20, 90, 135	2.6, 11.7, 17.5
	10	100	26
	15	30	11.7
	20	10, 25	5.2, 13
Intermediate	35	10, 20, 30	9.1, 18.2, 27.3
	40	15, 20, 30	15.6, 20.8, 31.2
	50	20	26
High	60	15, 20	23.4, 31.2
	70	15	27.3
	90	10, 15	23.4, 35.1
Chlorodifluoromethane (BP $\approx -40\,^{\circ}$C) was used as cryogen			
Low	5	45	5.8
	10	20, 30	5.2, 7.8
	20	15, 20, 30	7.8, 10.4, 15.6
Tetrafluoroethane (BP $\approx -26\,^{\circ}$C) was used as cryogen			

Cryogen was sprayed onto the comb through an electronically controlled standard automobile fuel injection valve positioned 4 cm from the surface at a 30° angle from the tissue normal. Cryogen spurt durations (τ) were set by a programmable digital delay

Table 2. Laser irradiation and CSC parameters used on each chicken comb. Chlorodifluoromethane was used on chicken combs 1–5; tetrafluoroethane on 6 and 7.

Chicken comb number	Delivered laser power, P (W)	Irradiation time, t_{irrad} (s)	Spurt duration, τ (ms)	Euthanasia time (post-experimental procedure)
1	20	10	0	1 h
	35	10, 20	50	
	40	30	50	
2	40	20	50, 80	3 d
	50	20	50, 80	
	60	20	50	
3	15	30	0	6 d
	40	15, 20, 30	50, 80	
	60	15	70	
	70	15	80	
	90	10, 15	100	
4	5	20, 90, 135	50, 60	8 d
	10	100	50	
	20	10, 25	0, 30, 50	
5	35	20, 30	50, 80	21 d
6	5	45	100	3 d
	10	30	100	
	15	10, 20, 30	0, 100	
	20	15	100	
7	10	20, 30	100	6 d
	15	15, 20	0, 100	
	20	20	100	

generator (DG535, Stanford Research Systems, Sunnyvale, CA), and ranged between 30 and 100 ms. The cooled site on the comb surface was concentric with the laser irradiated site, and about 10 mm in diameter. No indications of cryogen induced thermal injury were observed outside the laser irradiated site.

Radiometric measurement of surface temperature at the centre of the laser irradiated site was used to trigger the delivery of cryogen spurts. When the radiometric surface temperature reached a pre-specified threshold value (T_{thresh}; ranging between 36 and 41 °C), a cryogen spurt was delivered onto the comb. In this way, repetitive pulsed CSC during continuous laser irradiation was accomplished through a feedback system.

Infrared emission from the comb was detected using a 1 mm^2 liquid N_2 cooled HgCdTe detector (MDD-10E0-S1, Cincinnati Electronics, Mason, OH), optically filtered at the cold stop by a 10.6–14 μm bandpass filter. Because the infrared absorption coefficient of water in this range is approximately 60 mm^{-1} (Hale and Querry 1973), we expect that contributions to the infrared signal originate predominantly from superficial depths ($1/60\ mm^{-1} \approx 0.017$ mm).

The HgCdTe detector was placed at the focal plane of a 25 mm diameter $f/1$ Ge lens configured for unit magnification. For improved signal to noise ratio, the pupil was stopped to 5 mm diameter, and the infrared signal was amplitude modulated by turning

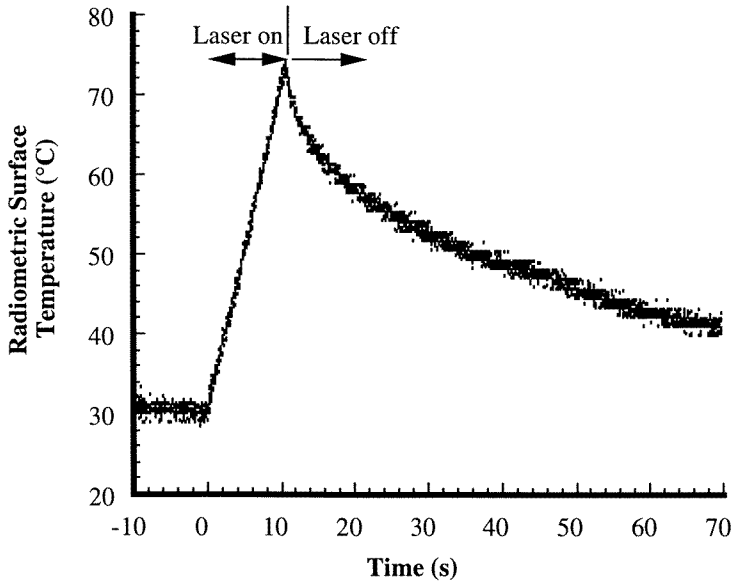

Figure 2. Radiometric surface temperature of the chicken comb in response to Nd:YAG laser irradiation ($P = 20$ W, $t_{\text{irrad}} = 10$ s, $d = 7$ mm) without CSC.

the detector on and off with a highly stable synthesized function generator (model DS345, Stanford Research Systems) at a rate of approximately 25 kHz. The modulated signal was synchronously detected by a lock-in amplifier (model SR850, Stanford Research Systems). The output signal of the lock-in amplifier was used to define the threshold trigger for the digital delay generator.

The infrared detection system was calibrated by measuring the lock-in amplifier output voltage as a function of the surface temperature of an aluminum block coated with highly emissive ($\varepsilon \approx 0.97$) black paint (TC-303 black, GIE Corp., Provo, UT) and heated by a resistive element from 23 to 75 °C. The surface temperature of the aluminum block was measured using a precision thermistor (8681, Keithley Instruments, Cleveland, OH) attached to the block; the measured output voltage varied linearly with temperature.

Following each experiment, irradiated and cooled sites were examined grossly for surface protection due to CSC, while the opposite sides of the combs were checked for blanching due to laser induced photocoagulation. Chickens were euthanized at various times (1 h–21 d) following the experiments (table 2). Combs were removed and prepared for histologic analysis.

3. Results and discussion

3.1. Temperature measurements

A recorded temperature measurement in response to laser irradiation ($P = 20$ W, $t_{\text{irrad}} = 10$ s) without CSC showed a linear increase in radiometric surface temperature to 75 °C on chicken 1 (figure 2). The observed linear increase indicates that both thermal diffusion and heat loss at the tissue surface–air interface were negligible during irradiation. Under these conditions, surface temperature is directly related to the radiant exposure, tissue thermal

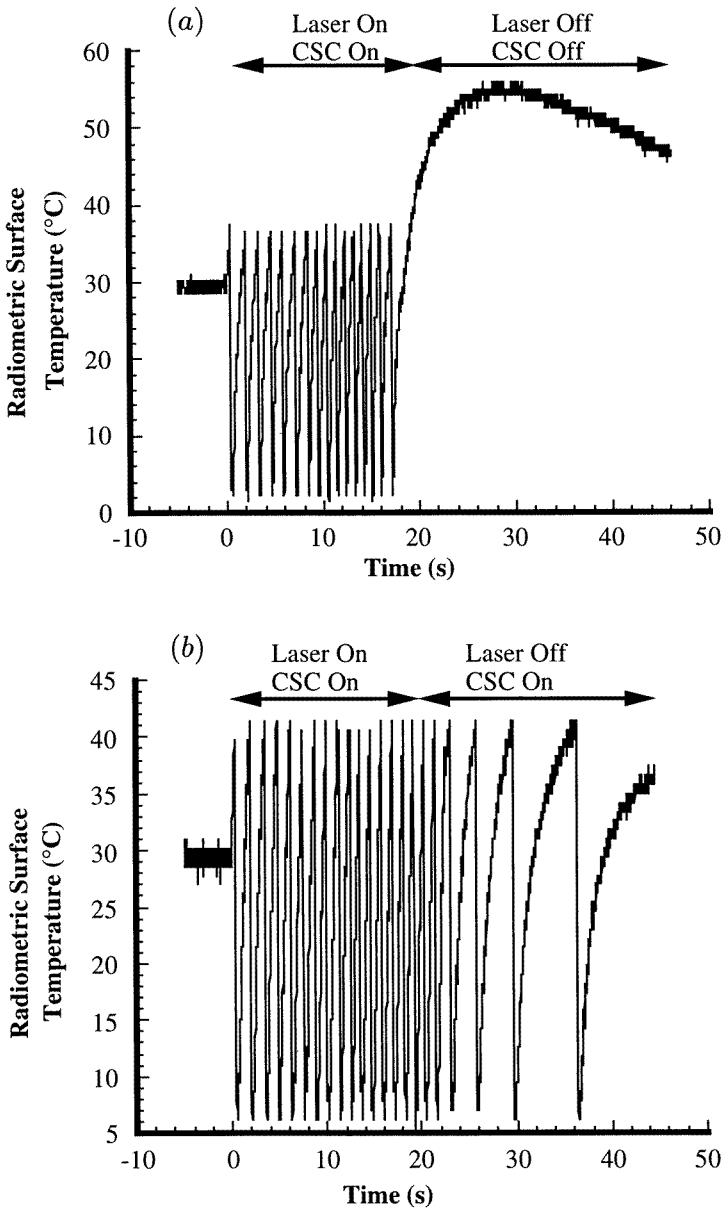

Figure 3. Radiometric surface temperature of the chicken comb in response to Nd:YAG laser irradiation ($P = 40$ W, $t_{irrad} = 20$ s, $d = 7$ mm) and 50 ms repetitive chlorodifluoromethane spurts. (*a*) CSC is off; (*b*) CSC is on after laser irradiation.

properties, and absorption coefficient (Welch and van Gemert 1995). Once the laser was turned off, surface temperature decreased monotonically. The comb surface cooled to its initial value after approximately 1 min.

Rapid surface temperature reductions to approximately 2 °C were observed in response to chlorodifluoromethane spurts ($\tau = 50$ ms) sprayed onto the comb during laser irradiation

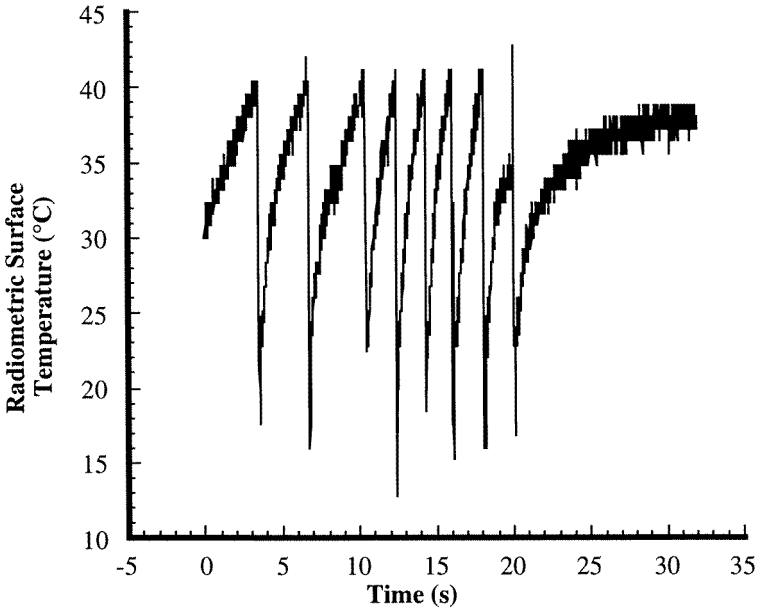

Figure 4. Radiometric surface temperature of the chicken comb in response to Nd:YAG laser irradiation ($P = 15$ W, $t_{\text{irrad}} = 20$ s, $d = 7$ mm) and 100 ms repetitive spurts of tetrafluoroethane.

($P = 40$ W, $t_{\text{irrad}} = 20$ s, $T_{\text{thresh}} = 36\,^{\circ}$C) (figure 3(*a*)). When the feedback system was turned off to prevent post-irradiation spurts, heat from within the comb diffused to the surface, and the surface temperature increased to 55 °C (figure 3(*a*)). However, when the feedback system remained on, cryogen spurts (with decreasing frequency) were delivered in response to heat diffusing from within the comb to the surface (figure 3(*b*)). With $T_{\text{thresh}} = 40\,^{\circ}$C for cryogen delivery, results indicate that 50 ms chlorodifluoromethane spurts consistently induced a temperature decrease of 34 °C.

With tetrafluoroethane, surface temperature was reduced to 13–23 °C in response to 100 ms spurts ($P = 15$ W, $t_{\text{irrad}} = 20$ s, $T_{\text{thresh}} = 41\,^{\circ}$C; figure 4). The variability in temperature reductions was due to the inconsistent cryogen spurts released from the reservoir used in our experiments. Due to the relatively higher BP of tetrafluoroethane (as compared to chlorodifluoromethane), sufficient cooling of superficial tissue structures at this comb site was not achieved, and photothermal injury ensued.

3.2. Gross observations

When using laser irradiation parameters specified in table 2, the irradiated combs always blanched in the absence of CSC. Photographs of chicken comb 1 irradiated and back surfaces are shown in figure 5(*a*) and (*b*), respectively. Laser irradiation parameters were $P = 35$ W, $t_{\text{irrad}} = 10$ s on site 1; $P = 35$ W, $t_{\text{irrad}} = 20$ s on sites 2 and 4; $P = 40$ W, $t_{\text{irrad}} = 30$ s on site 3; and $P = 20$ W, $t_{\text{irrad}} = 10$ s on site 5. CSC utilizing 50 ms chlorodifluoromethane spurts was applied to sites 1-4; post-laser irradiation spurts were delivered on site 4. Site 5 was irradiated in the absence of CSC. Tissue thickness was 4.7, 6.8, 5.9, 2.9, and 4.0 mm for sites 1–5, respectively.

(*a*)

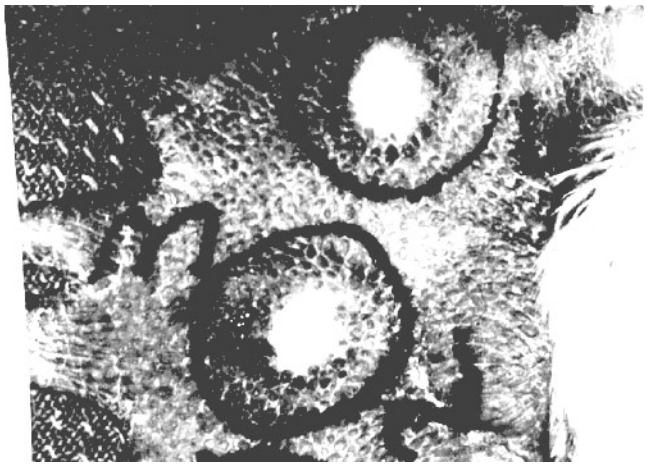

(*b*)

Figure 5. Photographs of (*a*) laser irradiated and (*b*) opposite surfaces of chicken comb number 1. CSC in conjunction with Nd:YAG laser irradiation was utilized on sites 1–4. Site 5 was irradiated without CSC. Cooled sites on the irradiated surface were not blanched. On the opposite side of the comb, sites 3 and 4 were blanched.

Although sites 1–4 on this chicken were irradiated with radiant exposures up to six times greater than that used on site 5 (the uncooled site), the surface of the comb on these locations was not blanched (figure 5(*a*)) since temperature was always maintained below a necessary threshold required for thermal damage. The opposite surfaces at sites 3 and 4, on the back side of the comb, however, were blanched (figure 5(*b*)), indicating a sufficient laser induced temperature increase was obtained at these locations to cause thermal damage. The opposite surfaces at sites 1, 2, and 5 were not blanched due to the combination of insufficient laser energy and greater tissue thickness at these locations.

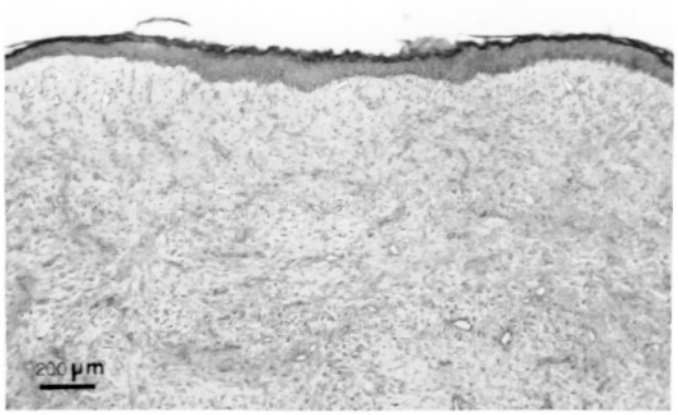

(*a*)

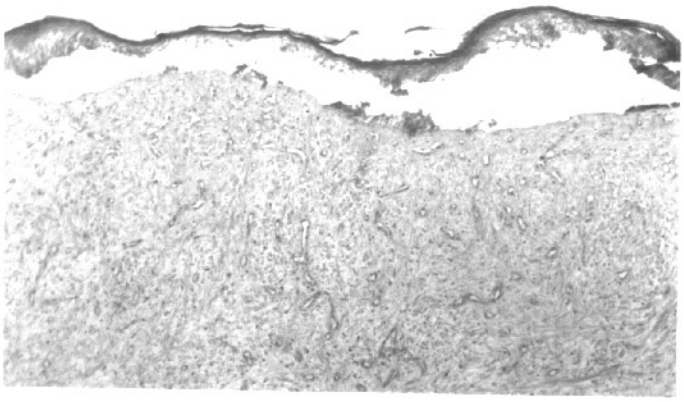

(*b*)

Figure 6. Histologic sections of chicken comb number 1 (euthanized 1 h after the experiment): (*a*) normal (non-irradiated and non-cooled) site, and (*b*) laser irradiated ($P = 20$ W, $t_{\text{irrad}} = 10$ s, $d = 7$ mm) and non-cooled site.

3.3. Histologic observations

A control site (non-irradiated and non-cooled) shows the normal chicken comb composite structure consisting of epidermis, papillary, and reticular dermis (figure 6(*a*)). Multiple vessels, having different lumen diameters, are present within the dermis. A histologic section obtained from site 5 of chicken number 1 (euthanized 1 h after the experiment) shows the detachment of epidermis in response to laser irradiation ($P = 20$ W, $t_{\text{irrad}} = 20$ s) without CSC (figure 6(*b*)).

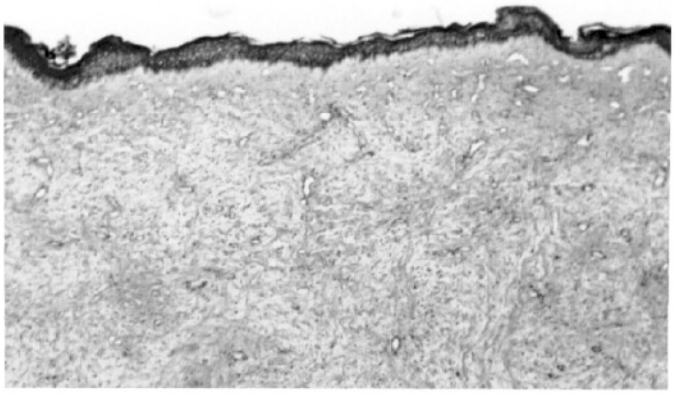

(*a*)

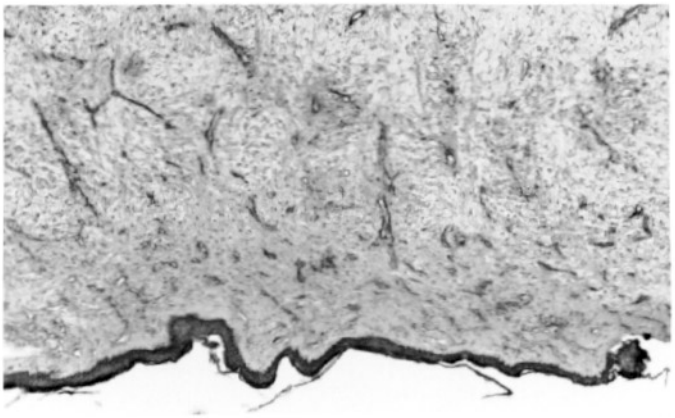

(*b*)

Figure 7. Histologic sections of chicken comb number 1 (euthanized 1 h after the experiment): (*a*) laser irradiated ($P = 35$ W, $t_{irrad} = 10$ s, $d = 7$ mm) and cooled (50 ms repetitive spurts of chlorodifluoromethane) site and (*b*) the opposite surface.

Histologic sections of chicken combs 1, 2, 4, and 5 irradiated in conjunction with CSC are shown in figures 7–10, respectively. Euthanasia time was 1 h and 3, 8 and 21 d; comb thickness was 2.9, 5.1, 4.2, and 4.0 mm on selected sites of the respective combs 1, 2, 4, and 5. Sections in figures 7(*a*)–10(*a*) show the comb structures on irradiated sites. The epidermis has remained intact due to CSC; papillary and reticular dermis are clearly distinguished.

Sections in figures 7(*b*)–10(*b*) show the opposite sides of the same combs. Most of the dermal vessels are occluded, and the necrotic tissue appears as a homogenous structure. Taken together, the results shown in figures 7–10 indicate that CSC was effective in protecting the epidermis and papillary dermis from thermal injury while achieving photocoagulation of the deeper tissue due to Nd:YAG laser irradiation.

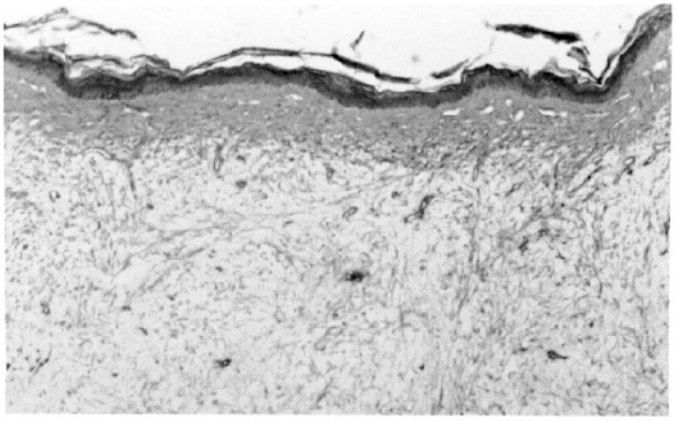

(*a*)

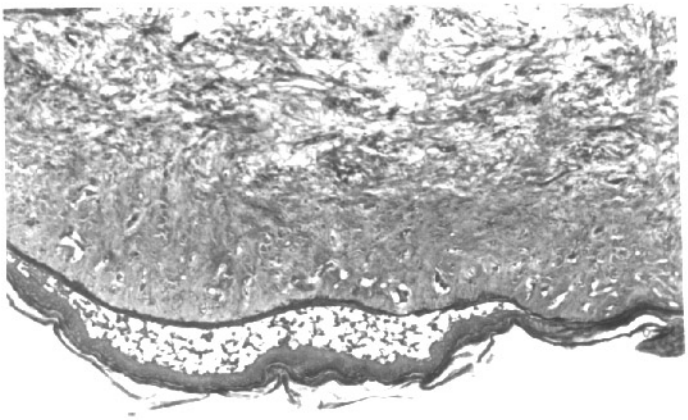

(*b*)

Figure 8. Histologic sections of chicken comb number 2 (euthanized 3 d after the experiment): (*a*) laser irradiated ($P = 50$ W, $t_{\text{irrad}} = 20$ s, $d = 7$ mm) and cooled (50 ms repetitive spurts of chlorodifluoromethane) site and (*b*) the opposite surface.

3.4. Effects of various laser irradiation and CSC parameters

With chlorodifluoromethane as the cryogen, protection of superficial tissues was achieved when irradiating the comb surface at low and intermediate power levels. However, the opposite surface of the comb was not blanched at low power levels (smallest thickness ≈ 5.5 mm) except when using $P = 20$ W and $t_{\text{irrad}} = 25$ s on a site that was 5.3 mm thick. The thickest comb site that was blanched on the opposite surface in response to intermediate irradiation was 6.1 mm ($P = 40$ W, $t_{\text{irrad}} = 20$ s).

When irradiating the combs at high power levels, superficial tissues were protected with

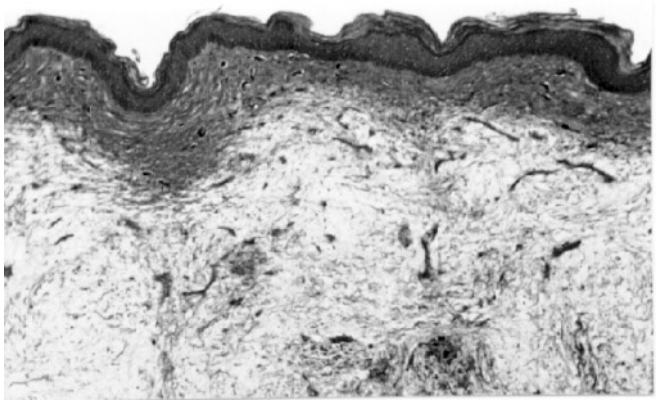

(*a*)

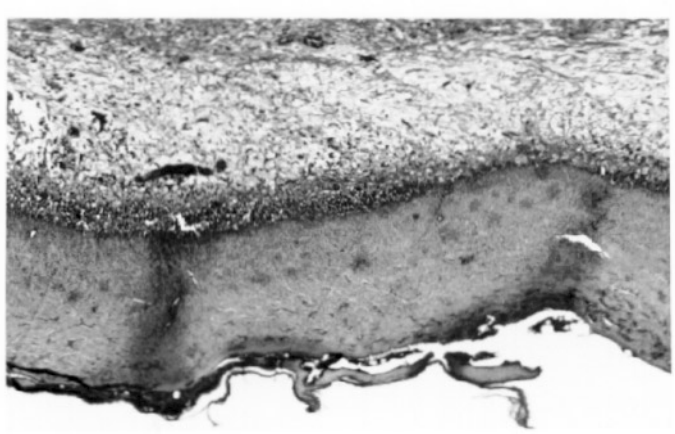

(*b*)

Figure 9. Histologic sections of chicken comb number 4 (euthanized 8 d after the experiment): (*a*) laser irradiated ($P = 20$ W, $t_{\text{irrad}} = 25$ s, $d = 7$ mm) and cooled (50 ms repetitive spurts of chlorodifluoromethane) site and (*b*) the opposite surface.

$P = 60$ W and $t_{\text{irrad}} = 15$ s. The thickest comb site that was blanched on the opposite surface in response to high-power laser irradiation was 7.5 mm ($P = 90$ W, $t_{\text{irrad}} = 15$ s); however, protection of superficial tissues was not attained.

With tetrafluoroethane as the cryogen, protection of superficial tissues was achieved when irradiating comb surfaces at $P = 5$ and 10 W. However, with these power levels, and their corresponding irradiation times (given in table 1), the opposite surfaces of the combs (smallest thickness ≈ 5.2 mm) were not blanched. Protection of superficial tissues was not possible when irradiating comb surfaces at $P = 15$ W while spray cooling with tetrafluoroethane. The thickest comb site that was blanched on the opposite surface was 4.8 mm ($P = 20$ W and $t_{\text{irrad}} = 15$ s).

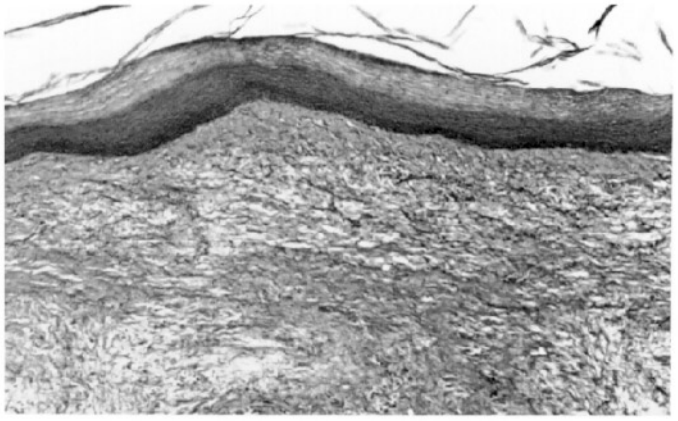

(*a*)

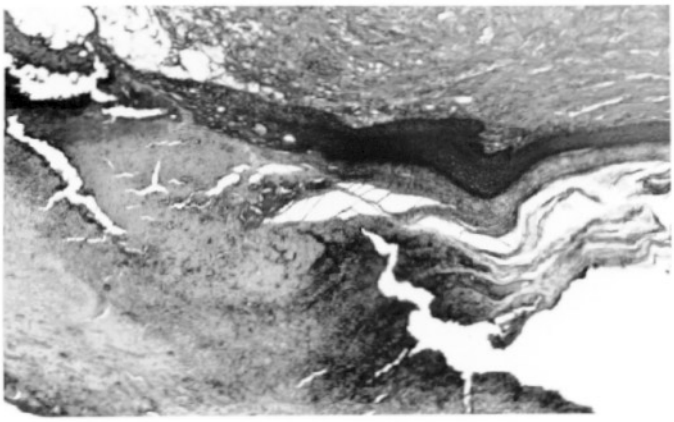

(*b*)

Figure 10. Histologic sections of chicken comb number 5 (euthanized 21 d after the experiment): (*a*) laser irradiated ($P = 35$ W, $t_{\text{irrad}} = 20$ s, $d = 7$ mm) and cooled (50 ms repetitive spurts of chlorodifluoromethane) site and (*b*) the opposite surface.

3.5. Cryogen spurt frequency (f_{spurt}) during and after laser irradiation

A close examination of figures 3(*b*) and 4 reveals that cryogen spurt frequency, $f_{\text{spurt}}(t)$ (Hz), increases during irradiation time, indicating that more heat diffuses to the surface as the internal temperature of the comb increases. f_{spurt} decreases with time after the laser is turned off (figure 3(*b*)). An analytical expression to predict f_{spurt} during and after laser irradiation is given as (see the appendix for the derivation)

$$f_{\text{spurt}}(t) = \begin{cases} C[1 - P(\tilde{\mu}_{\text{eff}})] & \text{for } t \leqslant t_{\text{irrad}} \quad (1a) \\ C[P(\tilde{\mu}^{*}_{\text{eff}}) - P(\tilde{\mu}_{\text{eff}})] & \text{for } t \geqslant t_{\text{irrad}} \quad (1b) \end{cases}$$

where C (s^{-1}) is an empirical coefficient inversely proportional to thermal energy removed by each cryogen spurt, $\tilde{\mu}_{\text{eff}} = \mu_{\text{eff}}\sqrt{\alpha t}$, α (m^2 s^{-1}) is the tissue thermal diffusivity, t (s) is the elapsed time after the onset of irradiation, $\mu_{\text{eff}} = \sqrt{3\mu_a[\mu_a + \mu_s(1-g)]}$ is the

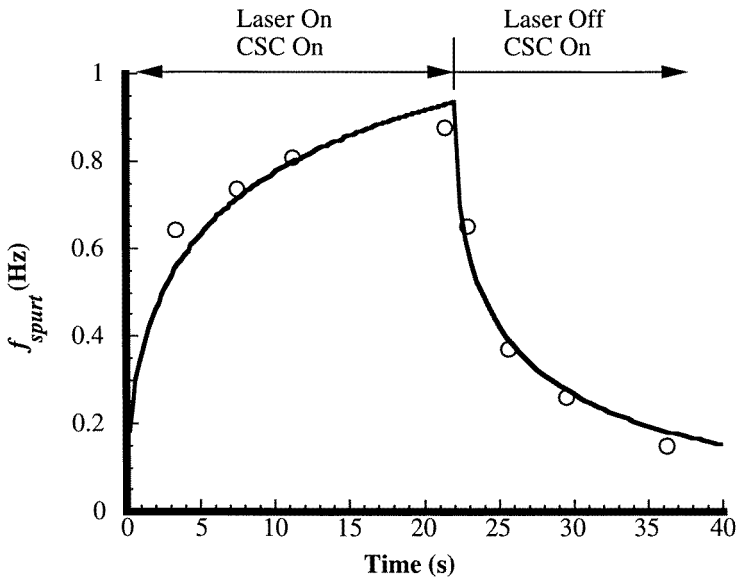

Figure 11. Theoretical (——) and experimental (○○○) values of cryogen spurt frequency during and after laser irradiation.

effective attenuation coefficient (m^{-1}), μ_a and μ_s (m^{-1}) are the tissue absorption and scattering coefficients, respectively, g is the anisotropy of scattering (Ishimaru 1989), $P(u) = e^{(u^2)}\text{erfc}(u)$, $\text{erfc}(u)$ is the complementary error function, $1 - \text{erf}(u)$, and $\tilde{\mu}^*_{\text{eff}} = \mu_{\text{eff}}\sqrt{\alpha(t - t_{\text{irrad}})}$.

Reasonably good agreement between theoretical and experimental values of f_{spurt} is obtained with $\mu_{\text{eff}} = 690\ m^{-1}$, $\alpha = 1.4 \times 10^{-7}\ m^2\ s^{-1}$ (the value for water), and $C = 1.5\ s^{-1}$ (figure 11). This value of μ_{eff} is comparable with a reported value for a highly vascularized tissue such as liver at 1064 nm ($\mu_{\text{eff}} = 750\ m^{-1}$; Hillgersberg *et al* 1993).

The experimental results shown in figure 11 represent the average values of f_{spurt} over various time intervals during and after laser irradiation ($P = 40$ W, $t_{\text{irrad}} = 20$ s). For example, the first experimental value of f_{spurt} shown in the figure represents the average over the first 3.4 s of irradiation, the second representing the average value over the next 4.0 s, etc. Similar fits could be obtained by changing μ_{eff} or α (independently by 50%), and adjusting C.

3.6. Clinical implications

Successful laser treatment of vascular birthmarks such as haemangiomas is based on photocoagulation of subsurface targeted tissue without thermal damage to the overlying epidermis. The light emitted from the Nd:YAG laser ($\lambda = 1064$ nm) penetrates deeply into the tissue, and has been used to photocoagulate thick haemangiomas (Rosenfeld and Sherman 1986, Apfelberg *et al* 1987, Rebeiz *et al* 1991). However, laser induced thermal damage to the epidermis remains a major concern (Achauer and Vander Kam 1988).

As demonstrated in experiments using the chicken comb animal model, epidermis protection and deep-tissue photocoagulation can be achieved by repetitive applications of a

short cryogen spurt during continuous Nd:YAG laser irradiation. In addition to protecting the superficial tissue structures from thermal injury, CSC can potentially reduce the irradiation time during laser treatment of haemangiomas. Relatively high incident powers (that might have otherwise resulted in photothermal destruction of superficial tissue) may be applied over a short time (e.g., 10–20 s).

Although in this study up to approximately 7 mm of tissue could be coagulated, successful treatment of haemangiomas might be achieved by inducing smaller coagulation depths to initiate the 'involution' process. Results of a clinical study using repetitive pulsed CSC in conjunction with continuous Nd:YAG laser irradiation for treatment of haemangiomas will be reported.

4. Conclusions

Spatially selective photocoagulation of subsurface targeted blood vessels by repetitive applications of a short cryogen spurt during continuous Nd:YAG laser irradiation has been demonstrated in the chicken comb animal model. This procedure may be effective in treatment of thick haemangiomas which requires photocoagulation of subsurface blood vessels while protecting the epidermis.

Acknowledgments

This work was supported by Institute of Arthritis and Musculoskeletal and Skin Disease (1R29-AR41638-01A1, R15-AR43403-01, and 1R01-AR42437-01A1) at the National Institutes of Health, National Science Foundation (BES-9634110), Whitaker Foundation Biomedical Engineering and Special Opportunity Grants, and SPIE Educational Grant in Optical Engineering. Technical assistance from Cheng Jen Chang and Binh Nguyen is greatly appreciated. The authors wish to thank Drs. Sol Kimel, Martin van Gemert, Lars O. Svaasand, and Derek Smithies for their valuable input.

Appendix. Derivations of equations (1*a*) and (1*b*)

The laser induced temperature increase within tissue can be computed by solving the heat diffusion equation:

$$\nabla^2 \Delta T_L(\boldsymbol{r}, t) + Q_L(\boldsymbol{r})/k = (1/\alpha)\partial \Delta T_L(\boldsymbol{r}, t)/\partial t \tag{A1}$$

where ΔT_L (°C) is the temperature increase due to absorption of laser light, k (W m^{-1} K^{-1}) and α (m^2 s^{-1}) are the tissue thermal conductivity and diffusivity, respectively, t (s) is the elapsed time after the onset of irradiation, $\boldsymbol{r}$ is the position vector in three-dimensional Cartesian coordinates. For a turbid medium, Q_L (W m^{-3}) can be approximated as

$$Q_L(\boldsymbol{r}) = \mu_a A_o(x, y) \exp(-\mu_{\text{eff}}\, z) \tag{A2}$$

where $A_o(x, y)$ (W m^{-2}) is related to irradiance and a factor that accounts for its augmentation at the surface due to back-scattering of light inside the tissue (Anderson *et al* 1989), x (m) and y (m) are distances along the tissue surface, z (m) is the distance into the tissue, μ_a (m^{-1}) is the tissue absorption coefficient, and μ_{eff} (m^{-1}) is the effective tissue attenuation coefficient as defined in subsection 3.5.

Solution of equation (A1) for a semi-infinite medium with its surface temperature, $T(x = 0, y = 0, z = 0, t)$, and its initial temperature, $T(x, y, z, t = 0)$ both at a constant

value, T_i, is given as (Carslaw and Jaeger 1959)

$$\Delta T_L(\boldsymbol{r},t) = \frac{\mu_a \alpha}{k\pi^{3/2}} \int_0^t \mathrm{d}t' \int_{-\infty}^{+\infty} \int_{-\infty}^{+\infty} A_0(x', y')\, \mathrm{e}^{-(\tilde{x}-\tilde{x}')^2-(\tilde{y}-\tilde{y}')^2}\, \mathrm{d}\tilde{x}\, \mathrm{d}\tilde{y} \times \int_0^{\infty} \mathrm{e}^{-2\tilde{\mu}_{\mathrm{eff}}\tilde{z}'} [\mathrm{e}^{-(\tilde{z}-\tilde{z}')^2} - \mathrm{e}^{-(\tilde{z}+\tilde{z}')^2}]\, \mathrm{d}\tilde{z}' \tag{A3}$$

where $\tilde{x}$, $\tilde{y}$, $\tilde{z}$, and $\tilde{\mu}_{\mathrm{eff}}$ represent dimensionless variables

$$\tilde{x} = x/2\sqrt{\alpha t'} \tag{A4a}$$

$$\tilde{y} = y/2\sqrt{\alpha t'} \tag{A4b}$$

$$\tilde{z} = z/2\sqrt{\alpha t'} \tag{A4c}$$

$$\tilde{\mu}_{\mathrm{eff}} = \mu_{\mathrm{eff}}\sqrt{\alpha t'}. \tag{A4d}$$

Heat removed per unit area of tissue surface by CSC, $H_0(t)$ (W m^{-2}), is related to the longitudinal component (perpendicular to the surface) of the laser induced thermal flux vector, $q_{L_z}(x, y, z, t = 0)$ (W m^{-2}) as

$$H_0(t) = -q_{L_z}(x, y, z = 0, t) = -k \frac{\partial T_L(\boldsymbol{r}, t)}{\partial z}\bigg|_{z=0} = -\frac{\mu_a \sqrt{\alpha}}{\pi^{3/2}} \int_0^t \frac{\mathrm{d}t'}{\sqrt{t'}} I_1(\tilde{x}, \tilde{y}) I_2(\tilde{\mu}_{\mathrm{eff}}) \tag{A5}$$

where

$$I_1 = \int_{-\infty}^{+\infty} \int_{-\infty}^{+\infty} A_0(x', y')\, \mathrm{e}^{-(\tilde{x}-\tilde{x}')^2-(\tilde{y}-\tilde{y}')^2}\, \mathrm{d}\tilde{x}'\, \mathrm{d}\tilde{y}' \tag{A6}$$

$$I_2 = \int_0^{\infty} 2\tilde{z}'\, \mathrm{e}^{-\tilde{z}'^2-2\tilde{\mu}_{\mathrm{eff}}\tilde{z}'}\, \mathrm{d}\tilde{z}' = -\frac{\mathrm{d}}{\mathrm{d}\tilde{\mu}_{\mathrm{eff}}} \int_0^{\infty} \mathrm{e}^{-\tilde{z}'^2-2\tilde{\mu}_{\mathrm{eff}}\tilde{z}'}\, \mathrm{d}\tilde{z}' = -\frac{\sqrt{\pi}}{2} \frac{\mathrm{d}P(\tilde{\mu}_{\mathrm{eff}})}{\mathrm{d}\tilde{\mu}_{\mathrm{eff}}} \tag{A7}$$

and $P(u) = \mathrm{e}^{(u^2)}\mathrm{erfc}\,(u)$.

Equation (A6) cannot be evaluated unless $A_0(x', y')$ is specified. For a constant value of A_0, the integral is evaluated as $A_0\pi$.

Using equations (A5)–(A7), the expression $\mathrm{d}\tilde{x}'\, \mathrm{d}\tilde{y}'\, \mathrm{d}x\, \mathrm{d}y = \mathrm{d}\tilde{x}\, \mathrm{d}\tilde{y}\, \mathrm{d}x'\, \mathrm{d}y'$, and considering that the power density, P_d (power absorbed per unit area of laser irradiated site; W m^{-2}), is

$$P_d = \int_0^{\infty} Q_L(\boldsymbol{r}')\, \mathrm{d}z' = \frac{\mu_a A_0}{\mu_{\mathrm{eff}}} \tag{A8}$$

we find

$$H_0(t) = -\frac{\mu_{\mathrm{eff}}\sqrt{\alpha}}{2} P_d \int_0^t \frac{\mathrm{d}t'}{\sqrt{t'}} \frac{\mathrm{d}P(\tilde{\mu}_{\mathrm{eff}})}{\mathrm{d}\tilde{\mu}_{\mathrm{eff}}}. \tag{A9}$$

Changing the integration variable in equation (A9) to $\tilde{\mu}_{\mathrm{eff}}$, and noting that

$$\mathrm{d}\tilde{\mu}_{\mathrm{eff}} = (\mu_{\mathrm{eff}}/2)\sqrt{\alpha/t'}\, \mathrm{d}t' \tag{A10}$$

we obtain

$$H_0(t) = -P_d \int_0^{\tilde{\mu}_{\mathrm{eff}}(t)} \frac{\mathrm{d}P(\tilde{\mu}_{\mathrm{eff}})}{\mathrm{d}\tilde{\mu}_{\mathrm{eff}}}\, \mathrm{d}\tilde{\mu}_{\mathrm{eff}} = P_d\{1 - [P(\tilde{\mu}_{\mathrm{eff}}(t))]\}. \tag{A11}$$

Due to application of repetitive cryogen spurts during laser irradiation, the surface temperature oscillates with time. To maintain the average surface temperature constant at T_i by cryogen spurts, H_0 must be balanced by $f_{\mathrm{spurt}}(t)E_0$, where f_{spurt} is the spurt frequency, and E_0 (J m^{-2}) is the amount of heat removed from tissue by CSC. Therefore,

$$f_{\mathrm{spurt}}(t) = \frac{H_0(t)}{E_0} = C[1 - P(\tilde{\mu}_{\mathrm{eff}})] \qquad \text{for } t \leqslant t_{\mathrm{irrad}} \tag{A12}$$

where $C = P_d/E_0$ (s^{-1}) is the ratio of total laser power density to the heat removed by each cryogen spurt.

For $t \geqslant t_{\text{irrad}}$, (i.e., after the laser is turned off), the heat transfer rate out of the tissue surface is calculated by adding the effect of a negative source, $-Q_L(\boldsymbol{r})$, which is turned on at $t = t_{\text{irrad}}$. From equations (A11) and (A12), we obtain

$$f_{\text{spurt}}(t) = C[P(\tilde{\mu}^*_{\text{eff}}) - P(\tilde{\mu}_{\text{eff}})] \qquad \text{for } t \geqslant t_{\text{irrad}} \tag{A13}$$

where $\tilde{\mu}^*_{\text{eff}} = \mu_{\text{eff}}\sqrt{\alpha(t - t_{\text{irrad}})}$.

We note that CSC usually reduces the time averaged surface temperature, T_{av}, below the initial temperature, T_i. Hence, there will be an additional heat transfer rate, H_1 (W), given by (Carslaw and Jaeger 1959)

$$H_1 = ka(T_i - T_{av})/\sqrt{\pi\alpha t} \tag{A14}$$

where a (m^2) is the area on tissue surface maintained at T_{av}. This additional heat transfer rate will result in more frequent cryogen spurts initially, but will have negligible effect shortly afterwards.

References

Achauer B M and Vander Kam V M 1988 Capillary (strawberry mark) of infancy: comparison of argon and Nd:YAG laser treatment *Plast. Reconstr. Surg.* **84** 60–70

Anderson R R, Beck H, Bruggemann U, Farinelli W, Jacques S L and Parrish J A 1989 Pulsed photothermal radiometry in turbid media: internal reflection of backscattered radiation strongly influences optical dosimetry *Appl. Opt.* **28** 2256–62

Anvari B, Milner T E, Tanenbaum B S, Kimel S, Svaasand L O and Nelson J S 1995a Dynamic epidermal cooling in conjunction with laser treatment of port wine stains: theoretical and preliminary clinical evaluations *Lasers Med. Sci.* **10** 105–12

——1995b Selective cooling of biological tissues: application for thermally mediated therapeutic procedures *Phys. Med. Biol.* **40** 241–52

Anvari B, Tanenbaum B S, Milner T E, Kimel S, Svaasand L O, Nelson J S 1995c A theoretical study of the thermal response of skin to cryogen spray cooling and pulsed laser irradiation: implications for treatment of port wine stain birthmarks *Phys. Med. Biol.* **40** 1451–65

Anvari B, Tanenbaum B S, Milner T E, Tang K, Liaw L-H, Kalafus K, Kimel S and Nelson J S 1996 Spatially selective photocoagulation of biological tissues: a feasibility study utilizing cryogen spray cooling *Appl. Opt.* **35** 3314–20

Apfelberg D B, Smith T, Lash H, White D N and Maser M R 1987 Preliminary report on use of the neodymium–YAG laser in plastic surgery *Lasers Surg. Med.* **7** 189–98

Berlien H P, Waldschmidt J and Müller G 1987 Laser treatment of cutan and deep vessel anomalies *Optoelectronics in Medicine* vol 87, ed W Waidelich and Hrsg Waidelich (New York: Springer) pp 526–8

Carslaw H S and Jaeger J C 1959 *Conduction of Heat in Solids* 2nd edn (Oxford: Clarendon)

Chess C and Chess Q 1993 Cool laser optics treatment of large telangiectasia of the lower extremities *J. Dermatol. Surg. Oncol.* **17** 74–80

Dreno B, Patrice T, Litoux B and Barriere H 1985 The benefit of chilling in argon laser treatment of port wine stains *Plast. Reconstr. Surg.* **74** 42–5

Gilchrest B A, Rosen S and Noel J M 1982 Chilling port wine stains improves the response to argon laser therapy *Plast. Reconstr. Surg.* **69** 279–83

Hale G M and Querry M R 1973 Optical constants of water in the 200 nm to 200 μm wavelength region *Appl. Opt.* **12** 555–63

Hillegersberg R, Pickering J W, Aalders M and Beek J F 1993 Optical properties of rat liver and tumor at 633 nm and 1064 nm: photofrin II enhances scattering *Lasers Surg. Med.* **13** 31–9

Ishimaru A 1989 Diffusion of light in turbid material *Appl. Opt.* **28** 2210–15

Kanakidou M, Dentener F J and Crutzen P J 1995 A global three-dimensional study of the fate of HCFCs and HFC-134a in the troposphere *J. Geophys. Res.* **100** 18 781–801

Manzer L E 1990 The CFC–ozone issue: progress on the development of alternatives to CFCs *Science* **249** 31–5

Mulliken J B and Young A E 1988 *Vascular Birthmarks: Hemangiomas and Malformations* (Philadelphia, PA: Saunders)

Nelson J S, Milner T E, Anvari B, Tanenbaum B S, Kimel S, Svaasand L O and Jacques S L 1995 Dynamic epidermal cooling during pulsed laser treatment of port wine stain—a new methodology with preliminary clinical evaluation *Arch. Dermatol.* **131** 695–700

Nelson J S, Milner T E, Anvari B, Tanenbaum B S, Svaasand L O and Kimel S 1996 Dynamic epidermal cooling in conjunction with laser-induced photothermolysis of port wine stain blood vessels *Lasers Surg. Med.* **19** 224–9

Orenstein A, Nelson J S, Liaw L-H, Kaplan R, Kimel S and Berns M W 1990 Photochemotherapy of hypervascular dermal lesions: a possible alternative to photothermal therapy? *Lasers Surg. Med.* **10** 334–43

Rebeiz E, April M M, Bohigian R K and Shapshay S M 1991 Nd–YAG laser treatment of venous malformations of the head and neck: an update *Otolaryngol. Head Neck Surg.* **105** 655–61

Rosenfeld H and Sherman R 1986 Treatment of cutaneous and deep vascular lesions with the Nd:YAG laser *Lasers Surg. Med.* **6** 20–4

Sturesson C and Andersson-Engels S 1996 Mathematical modelling of dynamic cooling and pre-heating, used to increase the depth of selective damage to blood vessels in laser treatment of port wine stains *Phys. Med. Biol.* **41** 413–28

Welch A J and van Gemert M J C 1995 *Optical–Thermal Response of Laser-Irradiated Tissue* (New York: Plenum) p 906

Werner J A, Lippert B M, Hoffmann P and Rudert H 1995 Nd:YAG laser therapy of voluminous hemangiomas and vascular malformations *Adv. Oto Rhino Laryngol.* **49** 75–80